Design, Modeling and Adaptive Force Control of a New Mobile Manipulator with Backlash Disturbances

Hami Tourajizadeh*
Department of Mechanical Engineering, Faculty of Engineering,
University of Kharazmi, Tehran, Iran
E-mail: Tourajizadeh@khu.ac.ir
*Corresponding author

Samira Afshari
Department of Mechanical Engineering, Faculty of Engineering,
University of Kharazmi, Tehran, Iran
E-mail: s.afshari90@yahoo.com

Abstract: In this paper a new model of the mobile robot is designed and modelled equipped by a manipulator which can perform an operational task. Also an adaptive force controller is designed and implemented on the robot to provide the capability of the operational task of the robot. Kinematic and kinetic modelling of the robot is developed and a new force control method is proposed for controlling the manipulator of the mobile robot by which the external disturbances caused by its operational performance can be controlled. Therefore, in this paper, a new mobile robot is designed which is suitable for operational tasks like firing and its related modelling is presented. Afterwards, an adaptive force controller is designed and implemented in order to neutralize the destructive effect of the mentioned backlash disturbance. By conducting some analytic and comparative simulation scenarios, the correctness of modelling and efficiency of the designed force controller is verified and it is shown that the proposed closed loop mobile manipulator can successfully accomplish a firing operation in a large workspace of a mobile robot with good accuracy.

Biographical notes: Hami Tourajizadeh received his PhD from IUST in the field mechanics, branch of control and robotics. More than 35 journal papers, 15 conference papers, 1 published book, 1-chapter book and 2 booked inventions are the results of his researches so far. He has been involved in teaching and research activities for more than 10 years in different universities and he is now an assistant professor of Kharazmi University since 2013. His research interests include robotics, automotive engineering, control and optimization. **Samira Afshari** is now an MSc student of Kharazmi University in the field of applied mechanical design. Her research interests include robotic systems and control methods.

1   INTRODUCTION

Mobile manipulators are nowadays widely applicable in civil and industries. Some of them are employed vastly as inspector of different environments in which the possibility or safety of human maneuver is not possible. In these mobile robots, some sensors are installed on the end-effector of the robot to move through some installations and verify the situation of the environment or measure the value of a specific parameter. In-pipe inspection robots are the most famous example of this kind of robots. The modified versions of these robots have manipulator and are able to perform operational tasks. In some operational applications, a variable force effects on the end-effector of the manipulator. This phenomenon can be observed in some processes like firing and every manipulator which is supposed to fire any object toward a specified target and this firing produces a backlash force on the chassis of the mobile robot. This backlash force which is not constant, affects the accuracy of the end-effector and its firing precision. Considering the mentioned force as an external disturbance, the accuracy of the firing should be assured using a proper force controller.

Mobile robots, inspection robots, and mobile manipulators are frequently studied so far in the literature, and different kind of them are modeled, controlled and manufactured. Jakubiak et al., proposed a new method to model the kinematics of such robots. A specific Jacobian inverse kinematics algorithm was introduced in this study. It has been applied to the unicycle-type mobile robot, and it has been shown that the algorithm performs efficiently unless the unicycle moves along a straight line trajectory [1].

In another paper by Trojnacki and Dąbek, longitudinal motion of a lightweight wheeled mobile robot on soft ground is noticed. The study is focused on the influence of the desired longitudinal velocity of a robot on both the longitudinal slip of the wheels and the ratio of wheel-terrain contact angles [2]. Khanpoor et al. considered trajectory tracking of a wheeled mobile robot towing an omnidirectional trailer. Kinematic and kinetic models were obtained, and then by combining these equations, an appropriate state space model has been introduced. Finally, a Lyapunov-based control algorithm was also proposed [3]. In another article by Sharma, and Panwar, kinematic and dynamic model of a mobile robot was derived using Lagrangian formulation and then sliding mode controller has been presented for the trajectory tracking of the wheeled mobile robot [4].

Hassanzadeh et al., studied mobile robot path planning in partially unknown environments proposing a method based on the shuffled frog leaping (SFL) optimization algorithm [5]. Integrated kinematic and dynamic

trajectory tracking control problem of wheeled mobile robots (WMRs) was also addressed by Shojaei et al. An adaptive robust tracking controller for WMRs[1] is proposed to cope with both parametric and nonparametric uncertainties in the robot model [6]. Also, a new nonlinear robust trajectory tracking control law for a non-holonomic mobile robot was presented by Chen et al. [7].

Comparison between a kinematic controller and an adaptive dynamic controller with consideration of unknown model parameters of a mobile robot was considered in research by Koubaa et al. [8]. The mentioned researches study the model of a simple mobile robot however in most cases a manipulator needs to be installed on a mobile robot to inspect or manipulate some special task. In a general approach, a symbolic algorithm, capable of deriving the equations of motion of N-rigid link manipulators with revolute-prismatic (R-P) joints, which is mounted on a mobile platform was presented by M. Korayem et al. [9].

E. Seidi et al., presented dynamic modeling and parametric analysis of nonholonomic wheeled mobile robotic manipulators applying the recursive Gibbs-Appell (G–A) approach [10]. Continuing research about the mobile manipulators, a general formulation as well as experimental studies for finding Maximum Allowable Dynamic Load (MADL) of non-holonomic Wheeled Mobile Manipulator (WMM) in the presence of obstacles and moving boundary condition has been presented by M. Korayem et al. [11]. The same author proposed a new solution to the problem of dynamic modeling of wheeled mobile manipulators with dual arms in an automatic and systemic approach. These kinds of robotic systems have agricultural applications such as pruning and fruit picking from trees [12].

Proper motion planning algorithms are the other necessary fields to be studied by researchers for intelligent robotic systems in order to execute their specific tasks. Considering this problem, some researches have been done by B. Deepak et al., introducing the inverse kinematic models for mobile manipulators [13]. operational tasks of the robots usually cause implementing a time-dependent or undetermined force on the tool of the manipulator that may not be generally desirable. This force which is usually considered as a disturbance should be neutralized properly using a suitable controller to maintain the desired accuracy of the manipulation process. For the mentioned studies, the implemented force is usually supposed to be determined according to the task of the robot, and it can be considered as the dynamics of the system. In some applications, the external implemented force on the manipulator has to be considered as disturbance since its time function is not predefined. In

---

[1] Wheeled mobile robots

these cases, a robust controller needs to be designed to assure the stability of the system. Some researchers have studied different algorithms of force control for different plants. A robust controller has been presented by M. Boukens et al., to be applied to a class of non-holonomic electrically driven mobile robots in order to neutralize the external disturbances and the effects of coupling terms between the mechanical subsystem and the electrical subsystem [14]. Omnidirectional mobile manipulators have been noticed by S. Djebrani et al., and a new approach based on the kinematic command structure and impedance control technique was presented in order to control these kinds of robotic systems. The additional task concept is used to solve the control problem of these redundant holonomic systems by taking into account the external forces [15]. The dynamic model of a UAV[2] with an attached robotic arm was derived in a symbolic matrix form through the Euler-Lagrangian formulation in a research done by V. Lippiello, and F. Ruggiero.

A Cartesian impedance control, which provides a dynamic relation between the generalized external forces acting on the structure and the system motion, was also designed. The hovering control of a quadrotor, equipped with a 3-DOF robotic arm which is subject to contact forces and external disturbances, has been tested in a simulated case study [16]. An adaptive position tracking system and a force control strategy were developed by Y. Wang et al., for a non-holonomic mobile manipulator robot, which combines the merits of Recurrent Fuzzy Wavelet Neural Networks (RFWNNs) [17].

A robust adaptive control method has systematically been proposed in a paper by X. Yin, and L. Pan to significantly reduce the tracking errors of 6 degrees of freedom (DOF) industrial robots under both external disturbances and parametric uncertainties. The control law was designed by combining the robust and adaptive capabilities to track the desired trajectory of the end-effector with sufficient robustness and accuracy in the presence of unknown external disturbances and parametric uncertainties [18]. In another study by L. Gracia et al., a hybrid position-force control of robots has been presented in order to apply surface treatments such as polishing, grinding, finishing, deburring, etc. The robot force control is designed using sliding mode concepts to increase its robustness [19]. A specific sub-group of the mobile manipulators which are supposed to perform an operational task is manipulator with a firing tool attached on the end-effector of the robot. These robots are widely applicable in both military and civil industries. Autonomous firing equipment of military systems, all of the automatic firing devices which are used in civil engineering like automatic rebar tying

machine, etc. are some examples of this kind of manipulators. The main challenge of this kind of mobile robot systems is the unwanted backlash force implemented on the end-effector tool during the firing. If this disturbing force could not be neutralized effectively, it can significantly affect the accuracy of its targeting. Few types of research are devoted for modeling of such systems and controlling the mentioned disturbing force. Fedaraviciu et al. studied the dynamics of a system considering this kind of forces and its effect on the position errors is investigated while a suspension system is also considered for its modeling [20]. In this research the modeling of the mobile manipulator is improved for performing firing operations and a proper suspension system is also added for promoting its modeling. However, no remedy is proposed here for controlling the disturbing force associated with firing moment of the device.

It can be seen that a mobile manipulator with six DOFs manoeuvrability is not designed and modelled which is vastly applicable for some application like firing. Also force control is not yet implemented on firing autonomous devices which is a significant and necessary improvement for increasing their targeting accuracy. According to the mentioned literature, it is proposed in this paper to implement an adaptive based force control system on a mobile manipulator which is responsible to perform a firing task. This controller guarantees the stability of the mobile manipulator during the firing process. In this approach, the firing force is considered as an external force. As a result, the computed torque method can be improved in the presence of firing disturbance force through which not only the position tracking of the manipulator can be satisfied, but also the required extra torque of the motors can be estimated to control the disturbing firing force and consequently the accuracy of the targeting process can be increased. To cover the mentioned mission, in the next section of the paper, the modeling of the required mobile manipulator is presented considering both kinematics and kinetics of the system. Afterward in section three, the scheme of the proposed adaptive control is presented which is based on the adaptive control and the designed controller is implemented on the robot dynamics. In section four, the correctness of robot modeling and also the efficiency of the proposed controller for the firing robot is verified by the aid of performing some analytic and comparative simulations conducted in MATLAB-SIMULINK. It is shown that using the mentioned model of the closed-loop mobile robot any kind of operational tasks including firing operations can be performed successfully while the proposed force controller guarantees its stability and targeting accuracy during the firing moments.

---

[2] unmanned aerial vehicle

2　DESIGN AND MODELING THE FIRING MOBILE MANIPULATOR

The proposed mobile manipulator in this paper is as depicted in "Fig. 1". This robot consists of a wheeled mobile robot with four wheels through which can be fitted on the rails and move along a straight line as expected. Two wheels of the mobile robot are drive wheels. Since the robot is supposed to move along a determined rail, the chassis itself has just one degree of freedom "x" for which can be controlled using one controlling input i.e. angular velocity of the drive wheels "w" which is the same for both of the right and left wheels since the robot does not need to rotate.
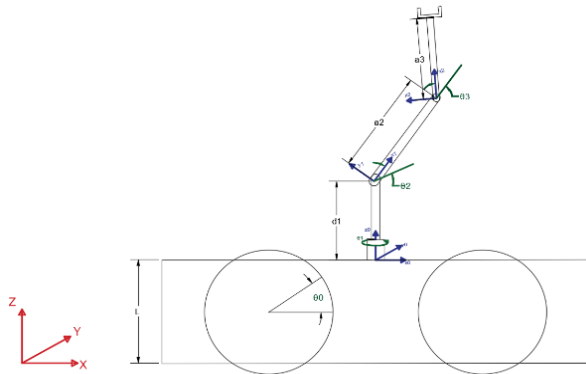
Fig. 1　　Schematic view of the mobile manipulator.

The robot can reach to the operation location by the aid of the mentioned mobile chassis and to perform its operational task within its spatial workspace, a linkage manipulator consisting three rotational generalized coordinates needs to be mounted on the mobile chassis. These three links can be moved within the 3D space by the aid of its three rotational actuators. Thus the engaged workspace of the end-effector and its related controlling joint space can be summarized as follow:

Work space DOFs: $\{x, y, z, \psi, \theta, \varphi\}$
Joint space Inputs: $\{\theta_0. \theta_1. \theta_2. \theta_3. \theta_4. \theta_5. \theta_6\}$

2.1. Kinematics

Using D-H parameterization [21], the related D-H table ("Table 1") can be extracted as:

Table 1 D-H parameters of the manipulator

link	a_i	α_i	d_i	θ_i
1	0	$\frac{\pi}{2}$	d_1	θ_1^*
2	a_2	0	0	θ_2^*
3	a_3	$\frac{\pi}{2}$	0	θ_3^*
4	0	$\frac{\pi}{2}$	0	θ_4^*
5	0	$-\frac{\pi}{2}$	0	θ_5^*
6	0	0	d_6	θ_6^*

Employing the mentioned D-H table results in the following position kinematics between the joint space and workspace of the robot:

$$
\begin{aligned}
x = r\theta_0 - d_6(&\sin\theta_1\sin\theta_4\sin\theta_5 \\
&+ \cos\theta_1 \cos\theta_4 \sin\theta_5 \cos(\theta_2 + \theta_3) \\
&- \cos\theta_1 \cos\theta_5 \sin(\theta_2 + \theta_3)) + a_2 \cos\theta_1 \cos\theta_2 \\
&+ a_3 \cos\theta_1 \cos(\theta_2 + \theta_3)
\end{aligned} \tag{1}
$$

$$
\begin{aligned}
y = d_6\big(&\sin\theta_5 \cos\theta_1 \sin\theta_4 \\
&- \sin\theta_5 \cos\theta_4 \sin\theta_1 \cos(\theta_2 + \theta_3) \\
&+ \cos\theta_5 (\cos\theta_2 \sin\theta_1 \sin\theta_3 \\
&+ \cos\theta_3 \sin\theta_1 \sin\theta_2)\big) \\
&+ \sin\theta_1(a_2 \cos\theta_2 + a_3 \cos(\theta_2 + \theta_3))
\end{aligned} \tag{2}
$$

$$
\begin{aligned}
z = l + d_1 &+ a_3 \sin(\theta_2 + \theta_3) + a_2 \sin\theta_2 \\
&- \frac{1}{2}d_6 \sin(\theta_2 + \theta_3) \sin(\theta_4 + \theta_5) \\
&- d_6 \cos\theta_5 \cos(\theta_2 + \theta_3) \\
&+ \frac{1}{2}d_6 \sin(\theta_4 - \theta_5) \sin(\theta_2 + \theta_3)
\end{aligned} \tag{3}
$$

$$
\begin{aligned}
\psi &= \tan^{-1}\left(\frac{a}{b}\right); \\
a &= - \cos\theta_5 \cos(\theta_2 + \theta_3) - \cos\theta_4 \sin\theta_5 \sin(\theta_2 + \theta_3) \\
b &= \sin\theta_6\sin\theta_5 \cos(\theta_2 + \theta_3) \\
&\quad - \cos\theta_4 \cos\theta_5 \sin(\theta_2 + \theta_3) \\
&\quad - \cos\theta_6 \sin\theta_4 \sin(\theta_2 + \theta_3)
\end{aligned} \tag{4}
$$

$$
\begin{aligned}
\theta = \sin^{-1}\big(&\cos\theta_6 \sin\theta_5 \cos(\theta_2 + \theta_3) \\
&- \sin(\theta_2 + \theta_3)(\cos\theta_6 \cos\theta_4 \cos\theta_5 - \sin\theta_4 \sin\theta_6)\big)
\end{aligned} \tag{5}
$$

$$
\begin{aligned}
\varphi &= \tan^{-1}\left(\frac{n \cos\theta_1 + c}{n \sin\theta_1 - d}\right); \\
n &= -\cos\theta_2 \cos\theta_3 \sin\theta_4 \sin\theta_6 + \cos\theta_2 \cos\theta_6 \sin\theta_3\sin\theta_5 + \\
&\quad \cos\theta_3 \cos\theta_6 \sin\theta_2 \sin\theta_5 + \sin\theta_2\sin\theta_3\sin\theta_4 \sin\theta_6 + \\
&\quad \cos\theta_2 \cos\theta_3 \cos\theta_4 \cos\theta_5 \cos\theta_6 - \\
&\quad \cos\theta_4 \cos\theta_5 \cos\theta_6 \sin\theta_2\sin\theta_3 \ ; \\
c &= \sin\theta_1 \cos\theta_4 \sin\theta_6 + \sin\theta_1 \cos\theta_5 \cos\theta_6 \sin\theta_4 \ ; \\
d &= \cos\theta_1 \cos\theta_4 \sin\theta_6 + \cos\theta_1 \cos\theta_5 \cos\theta_6 \sin\theta_4
\end{aligned} \tag{6}
$$

Where $x, y, z, \psi, \theta, \varphi$ are the global coordinates of the end-effector. Also the parameters $r, d_1, a_2, a_3, d_6, lr$ are

the radius of the wheels , length of the first link, length of the second link, length of the third link, length of the wrist and height of the mobile chassis, respectively. θ_0 is the first joint angle determining the rotation angle of the wheels. θ_1 is the second joint angle. θ_2 is the third joint angle. θ_3 is the fourth joint angle. Also $\theta_4, \theta_5, \theta_6$ are the joint angles related to the orientation of the wrist. In order to calculate the velocity kinematics of the system and extract the relation between the joint space speed of the motor and workspace velocity of the end-effector, Jacobian of the system needs to be solved:

$$J = \begin{bmatrix} \frac{\partial x}{\partial \theta_0} & \cdots & \frac{\partial x}{\partial \theta_6} \\ \vdots & \vdots & \vdots \\ \frac{\partial \varphi}{\partial \theta_0} & \cdots & \frac{\partial \varphi}{\partial \theta_6} \end{bmatrix} \qquad (7)$$

Thus we have:

$$\dot{p} = J\dot{q} \qquad (8)$$

Where:

$$\dot{p} = [\dot{x} \quad \dot{y} \quad \dot{z} \quad \dot{\psi} \quad \dot{\theta} \quad \dot{\varphi}]^T \qquad (9)$$

$$\dot{q} = [\dot{\theta}_0 \quad \dot{\theta}_1 \quad \dot{\theta}_2 \quad \dot{\theta}_3 \quad \dot{\theta}_4 \quad \dot{\theta}_5 \quad \dot{\theta}_6]^T \qquad (10)$$

Considering the fact that the system is over constrained, Pseudoinverse of the Jacobian matrix needs to be calculated in order to cover the inverse kinematics of the robot:

$$\dot{q} = J^T (JJ^T)^{-1} \dot{p} \qquad (11)$$

2.2. Dynamics

Lagrange method is used here to extract the dynamic model of the system. Since the robot is considered to be employed for firing operational tasks, the generalized coordinates related to the wrist is not required, and after removing the wrist, we have four joint variable $\theta_0, \theta_1, \theta_2, \theta_3$. Thus, the kinetic and potential energy of the system can be calculated as follows:

$$T_w = \frac{1}{2} m_w V_w{}^T V_w + \frac{1}{2} \omega_w{}^T I_w \omega_w \qquad (12)$$

$$U_w = m_w g(\frac{l}{2}) \qquad (13)$$

Where $T_w T_w$ and $U_w U_w$ are the kinetic and potential energy respectively for each wheel of the robot. Similarly, the kinetic energy is calculated for the other parts of the system separately. It is clear that the kinetic energy for the mobile chassis includes just translational one. The potential energy of each part can be calculated as follows:

$$U_b = m_b g(\frac{l}{2}) \qquad (14)$$

$$U_1 = m_1 g(l + \frac{d_1}{2}) \qquad (15)$$

$$U_2 = m_2 g(l + d_1 + \frac{a_2}{2} \sin \theta_2) \qquad (16)$$

$$U_3 = m_3 g(l + d_1 + a_2 \sin \theta_2 + \frac{a_3}{2} \sin(\theta_2 + \theta_3)) \qquad (17)$$

Where the index b indicates the mobile chassis and the numbers show the related links. Moreover, the kinetic energy of the related parts can be calculated as:

$$T_b = \frac{1}{2} m_b \{V_b\}^T \{V_b\} \qquad (18)$$

$$T_1 = \frac{1}{2} m_1 \{V_1\}^T \{V_1\} + \frac{1}{2} \{\omega_1\}^T [I_1]\{\omega_1\} \qquad (19)$$

$$T_2 = \frac{1}{2} m_2 \{V_2\}^T \{V_2\} + \frac{1}{2} \{\omega_2\}^T [I_2]\{\omega_2\} \qquad (20)$$

$$T_3 = \frac{1}{2} m_3 \{V_3\}^T \{V_3\} + \frac{1}{2} \{\omega_3\}^T [I_3]\{\omega_3\} \qquad (21)$$

Where the translational velocities of the links' center of mass can be calculated as:

$$V_w = V_b = V_1 = \begin{bmatrix} r\dot{\theta}_0 \\ 0 \\ 0 \end{bmatrix} \qquad (22)$$

$$V_2 = \frac{d}{dt} \left(\begin{bmatrix} \frac{a_2}{2} \cos \theta_2 \cos \theta_1 + r\theta_0 \\ \frac{a_2}{2} \cos \theta_2 \sin \theta_1 \\ d_1 + a_2 \sin \theta_2 \end{bmatrix} \right) \qquad (23)$$

$$V_3 = \frac{d}{dt} \left(\begin{bmatrix} c_1 \\ c_2 \\ c_3 \end{bmatrix} \right) ;$$

$$c_1 = (a_2 \cos \theta_2 + a_3 \cos(\theta_2 + \theta_3)) \cos \theta_1 + r\theta_0 \qquad (24)$$

$$c_2 = (a_2 \cos \theta_2 + a_3 \cos(\theta_2 + \theta_3)) \sin \theta_1$$

$$c_3 = d_1 + a_2 \sin \theta_2 + a_3 \sin(\theta_2 + \theta_3)$$

Also, the rotational velocities can be evaluated as:

$$\omega_w = \begin{bmatrix} 0 \\ -\dot{\theta}_0 \\ 0 \end{bmatrix} ; \quad \omega_b = \begin{bmatrix} 0 \\ 0 \\ 0 \end{bmatrix} \omega_w = \begin{bmatrix} 0 \\ -\dot{\theta}_0 \\ 0 \end{bmatrix} ; \quad \omega_1 = \begin{bmatrix} 0 \\ 0 \\ \dot{\theta}_1 \end{bmatrix} ;$$

$$\omega_2 = \begin{bmatrix} 0 \\ -\dot{\theta}_2 \\ \dot{\theta}_1 \end{bmatrix} ; \quad \omega_3 = \begin{bmatrix} 0 \\ -(\dot{\theta}_2 + \dot{\theta}_3) \\ \dot{\theta}_1 \end{bmatrix} \qquad (25)$$

Each part's moment of inertia is:

$$I_w = \begin{bmatrix} 0 & 0 & 0 \\ 0 & I_{wy} & 0 \\ 0 & 0 & 0 \end{bmatrix} \qquad (26)$$

$$I_1 = \begin{bmatrix} 0 & 0 & 0 \\ 0 & 0 & 0 \\ 0 & 0 & I_{1z} \end{bmatrix} \qquad (27)$$

$$I_2 = \begin{bmatrix} 0 & 0 & 0 \\ 0 & I_{2y} & 0 \\ 0 & 0 & I_{2z} \end{bmatrix} \qquad (28)$$

$$\begin{bmatrix} \cos\theta_0 & 0 & \sin\theta_0 \\ 0 & 1 & 0 \\ -\sin\theta_0 & 0 & \cos\theta_0 \end{bmatrix}$$

$$I_3 = \begin{bmatrix} 0 & 0 & 0 \\ 0 & I_{3y} & 0 \\ 0 & 0 & I_{3z} \end{bmatrix} \qquad (29)$$

Here, $\theta_0, \theta_1, \theta_2, \theta_3 \theta_0. \theta_1. \theta_2. \theta_3$ are the joint space variables and $\dot{\theta}_0, \dot{\theta}_1, \dot{\theta}_2, \dot{\theta}_3$ refer to the rotational velocities of these joints. m_w, m_b, m_1, m_2, m_3 are the mass of each wheel, mobile chassis, the first, the second and the third link, respectively. Similarly, d_1, a_2, a_3 are the length of the links. l l is the height of mobile chassis and also r r is the, wheel's radius, as mentioned before. Thus the total potential and kinetic energy of the system can be considered as the summation of the calculated energies. The Lagrangian function can now be established as:

$$L = T_{total} - U_{total} \qquad (30)$$

Where:

$$T_{total} = 4T_w + T_b + T_1 + T_2 + T_3 \quad ;$$
$$U_{total} = 4U_w + U_b + U_1 + U_2 + U_3 \qquad (31)$$

Thus, the dynamic equations of the system can be calculated by the aid of following differential equations [22]:

$$\frac{d}{dt}\left(\frac{\partial L}{\partial \dot{\theta}_0}\right) - \frac{\partial L}{\partial \theta_0} = \tau_0 \quad ;$$

$$\frac{d}{dt}\left(\frac{\partial L}{\partial \dot{\theta}_1}\right) - \frac{\partial L}{\partial \theta_1} = \tau_1 \quad ;$$

$$\frac{d}{dt}\left(\frac{\partial L}{\partial \dot{\theta}_2}\right) - \frac{\partial L}{\partial \theta_2} = \tau_2 \quad ;$$

$$\frac{d}{dt}\left(\frac{\partial L}{\partial \dot{\theta}_3}\right) - \frac{\partial L}{\partial \theta_3} = \tau_3 \qquad (32)$$

Where $\tau_0, \tau_1, \tau_2, \tau_3$ are the generalised forces of the robot which is the motor torque of the joints. Finally, the motion equations can be demonstrated as follows:

$$\tau = D\ddot{q} + C\dot{q} + G \qquad (33)$$

Where:

$$\tau = \begin{bmatrix} \tau_0 & \tau_1 & \tau_2 & \tau_3 \end{bmatrix}^T \quad ;$$
$$\dot{q} = \begin{bmatrix} \dot{\theta}_0 & \dot{\theta}_1 & \dot{\theta}_2 & \dot{\theta}_3 \end{bmatrix}^T \quad ;$$
$$\ddot{q} = \begin{bmatrix} \ddot{\theta}_0 & \ddot{\theta}_1 & \ddot{\theta}_2 & \ddot{\theta}_3 \end{bmatrix}^T \qquad (34)$$

D, C and G are inertia and Coriolis matrices and gravity vector respectively. These matrices are calculated as a function of the joint variables and their related velocities. The dimension of the resultant matrices and also their dependency on the joint variables can be demonstrated as follows:

$$D(q) = \begin{bmatrix} d_{11} & d_{12} & d_{13} & d_{14} \\ d_{12} & d_{22} & 0 & 0 \\ d_{13} & 0 & d_{33} & d_{34} \\ d_{14} & 0 & d_{34} & d_{44} \end{bmatrix} \quad ;$$

$$C(q,\dot{q}) = \begin{bmatrix} 0 & c_{12} & c_{13} & c_{14} \\ 0 & c_{22} & c_{23} & c_{24} \\ 0 & c_{32} & c_{33} & c_{34} \\ 0 & c_{42} & c_{43} & c_{44} \end{bmatrix} \quad ;$$

$$G(q,\dot{q}) = \begin{bmatrix} 0 \\ g_{21} \\ g_{31} \\ g_{41} \end{bmatrix} \qquad (35)$$

3 FORCE CONTROL SCHEME

The robot can be employed for two categories of repairing operations. The first category is related to the tasks in which the external force is exactly predetermined. Another application is associated with the processes in which the external force is unknown. In the former case, the external force can be modeled in the dynamics of the system and the impedance control method can ensure the stability and accuracy of the robot movement and its related operation. However, for the latter case, the external force is not specifically determined and inevitably needs to be considered as a disturbance. For our case of study in which a firing should be accomplished, the second approach will be realized for which adaptive force control is proposed in this paper.

3.1. Impedance Control
The state space of the model needs to be extracted before designing the model-based controllers, and its related controllability of the systems should be investigated. According to the dynamic "Eq. (33)", the nonlinear state space of the system will be:

$$\begin{cases}
\dot{x}_1 = x_2 \\
\dot{x}_2 = k_{11}(u_1 - c_{12}x_4 - c_{13}x_6 - c_{14}x_8) \\
+k_{12}(u_2 - c_{22}x_4 - c_{23}x_6 - c_{24}x_8 - g_{21}) \\
+k_{13}(u_3 - c_{32}x_4 - c_{33}x_6 - c_{34}x_8 - g_{31}) \\
+k_{14}(u_4 - c_{42}x_4 - c_{43}x_6 - c_{44}x_8 - g_{41}) \\
\dot{x}_3 = x_4 \\
\dot{x}_4 = k_{21}(u_1 - c_{12}x_4 - c_{13}x_6 - c_{14}x_8) \\
+k_{22}(u_2 - c_{22}x_4 - c_{23}x_6 - c_{24}x_8 - g_{21}) \\
+k_{23}(u_3 - c_{32}x_4 - c_{33}x_6 - c_{34}x_8 - g_{31}) \\
+k_{24}(u_4 - c_{42}x_4 - c_{43}x_6 - c_{44}x_8 - g_{41}) \\
\dot{x}_5 = x_6 \\
\dot{x}_6 = k_{31}(u_1 - c_{12}x_4 - c_{13}x_6 - c_{14}x_8) \\
+k_{32}(u_2 - c_{22}x_4 - c_{23}x_6 - c_{24}x_8 - g_{21}) \\
+k_{33}(u_3 - c_{32}x_4 - c_{33}x_6 - c_{34}x_8 - g_{31}) \\
+k_{34}(u_4 - c_{42}x_4 - c_{43}x_6 - c_{44}x_8 - g_{41}) \\
\dot{x}_7 = x_8 \\
\dot{x}_8 = k_{41}(u_1 - c_{12}x_4 - c_{13}x_6 - c_{14}x_8) \\
+k_{42}(u_2 - c_{22}x_4 - c_{23}x_6 - c_{24}x_8 - g_{21}) \\
+k_{43}(u_3 - c_{32}x_4 - c_{33}x_6 - c_{34}x_8 - g_{31}) \\
+k_{44}(u_4 - c_{42}x_4 - c_{43}x_6 - c_{44}x_8 - g_{41})
\end{cases} \quad (36)$$

Where:

$$x = \begin{bmatrix} x_1 \\ x_2 \\ x_3 \\ x_4 \\ x_5 \\ x_6 \\ x_7 \\ x_8 \end{bmatrix} = \begin{bmatrix} \theta_0 \\ \dot{\theta}_0 \\ \theta_1 \\ \dot{\theta}_1 \\ \theta_2 \\ \dot{\theta}_2 \\ \theta_3 \\ \dot{\theta}_3 \end{bmatrix}; \quad u = \begin{bmatrix} \tau_0 \\ \tau_1 \\ \tau_2 \\ \tau_3 \end{bmatrix} = \begin{bmatrix} u_1 \\ u_2 \\ u_3 \\ u_4 \end{bmatrix};$$

$$K = D^{-1}(q) = \begin{bmatrix} k_{11} & k_{12} & k_{13} & k_{14} \\ k_{21} & k_{22} & k_{23} & k_{24} \\ k_{31} & k_{32} & k_{33} & k_{34} \\ k_{41} & k_{42} & k_{43} & k_{44} \end{bmatrix} \quad (37)$$

Controllability of the system is locally investigated by linearizing the system around its operating point (x_0, u_0) and the related controllability matrix is formed then. By linearizing $\dot{x} = f(x, u)$ the linearized state space can be written as:

$$\dot{x} = Ax + Bu \quad (38)$$

For this case study and its related operating point we have:

$$A = \frac{\partial f}{\partial x}\Big|_{\substack{x=x_0 \\ u=u_0}} =$$

$$\begin{bmatrix}
0 & 1 & 0 & 0 & 0 & 0 & 0 & 0 \\
0 & 0 & 1.1875 & 0 & -4.0049 & 0 & 0.8202 & 0 \\
0 & 0 & 0 & 1 & 0 & 0 & 0 & 0 \\
0 & 0 & -1.0638 & 0 & -1.0770 & 0 & 0.0833 & 0 \\
0 & 0 & 0 & 0 & 0 & 1 & 0 & 0 \\
0 & 0 & 0.3059 & 0 & -3.8195 & 0 & -6.6578 & 0 \\
0 & 0 & 0 & 0 & 0 & 0 & 0 & 1 \\
0 & 0 & 0.7797 & 0 & 42.3584 & 0 & 36.7394 & 0
\end{bmatrix};$$

$$B = \frac{\partial f}{\partial u}\Big|_{\substack{x=x_0 \\ u=u_0}} =$$

$$\begin{bmatrix}
0 & 0 & 0 & 0 \\
10.0208 & 2.2445 & 1.1915 & 3.0368 \\
0 & 0 & 0 & 0 \\
2.2445 & 21.1653 & 0.2669 & 0.6802 \\
0 & 0 & 0 & 0 \\
1.1915 & 0.2669 & 29.5068 & -55.4458 \\
0 & 0 & 0 & 0 \\
3.0368 & 0.6802 & -55.4458 & 206.9782
\end{bmatrix} \quad (39)$$

The operating point is considered as follows:

$$x_0 = \begin{bmatrix} 0.45 & 0 & 0.45 & 0 & 0.45 & 0 & 0.45 & 0 \end{bmatrix}^T;$$
$$u_0 = \begin{bmatrix} 0 & 0 & 0 & 0 \end{bmatrix}^T \quad (40)$$

Then the controllability matrix could be calculated easily:

$$\varphi_c = $$
$$[B \quad AB \quad A^2B \quad A^3B \quad A^4B \quad A^5B \quad A^6B \quad A^7B] \quad (41)$$

Which is an 8×32 matrix. Considering the rank of this matrix that is 8, the controllability of the system is guaranteed locally around the operating point specified before.

Since a mobile manipulator is a nonlinear dynamic system, firstly, the inverse dynamic method is used in order to control the robot. Thus, using the inverse dynamics of the system, the following motors' torque is required to provide the desired path:

$$u = D(q_d)\ddot{q}_d + C(q_d, \dot{q}_d)\dot{q}_d + G(q_d, \dot{q}_d) \quad (42)$$

Where $q_d, \dot{q}_d$ are relatively the desired time varying path of position and velocity of the joint space vector, q. In order to control the robot in a regulation or trajectory tracking, Feed-back Linearization (F.L.) controller can be applied by the following input torque vector [22]. Since all of the nonlinear rows of the state space have a controlling input, it is possible to linearize the system using F.L. and to control the states using pole placement method by proper determination of the controlling gains.

$$u = D(q)(\ddot{q}_d - 2\Lambda\dot{e} - \Lambda^2 e) + C(q, \dot{q})\dot{q} + G(q, \dot{q}) \quad (43)$$

Where Λ is a 4×4 diagonal matrix including the controlling gains which can be determined considering the desired poles of the closed-loop system. The actual error dynamic of the system will be then:

$$\ddot{e} + 2\Lambda\dot{e} + \Lambda^2 e = 0 \qquad (44)$$

Afterward, because the robot is supposed to be used for operational tasks, an external force will be implemented on the end-effector of the robot. This force needs to be neutralized in order to provide an accurate regulation or tracking during the operational task. Therefore, the Feed-back Linearization control can be improved as Impedance control method by defining the following required input torque [23].

$$u = D(q)(\ddot{q}_d - 2\Lambda\dot{e} - \Lambda^2 e) + C(q,\dot{q})\dot{q} \\ + G(q,\dot{q}) + J^T F \qquad (45)$$

The added term of $J^T F$ calculates the required torque of the robot motors for bearing the external force of F, which is considered here as follows:

$$F = [F_x \quad F_y \quad F_z \quad M_x \quad M_y \quad M_z]^T \qquad (46)$$

Here, F_x is the force applied to the end-effector in the positive direction of the global X axis. similarly, F_y and F_z are the forces in the positive direction of global Y and Z axes, respectively. As the same way, M_x, M_y, M_z are the torques applied about the direction of three global system's axes. Thus if the external force functionality is determined, it will be possible to control the force and position of the manipulator simultaneously, using the mentioned controlling input.

3.2. Proposed Adaptive Force Control

Here it is supposed that the external force which is the result of firing action cannot be exactly determined as a function of time and it is required to be considered as a disturbing external force. Thus it is supposed to improve the accuracy of the robot performance using a proper adaptive control [22]. This process can modify the predicted applied force and improve the accuracy of targeting.

Therefore, for firing case in which the force cannot be explained as a predetermined function, the following adaptive controlling force is proposed in which the nominal values of the force need to be initially guessed by the operator considering the nature of the operation:

$$u = D(q)(\ddot{q}_d - 2\Lambda\dot{e} - \Lambda^2 e) + C(q,\dot{q})\dot{q} \\ + G(q,\dot{q}) + J^T \hat{F} \qquad (47)$$

Where $\hat{F}$ is the nominal external force and torque vector which should be estimated initially by the operator. In order to evaluate this nominal value, Lyapunov stability

is employed here [22]. By applying the mentioned input, the dynamic equation of the error will be as follows:

$$D(q)(\ddot{e} + 2\Lambda\dot{e} + \Lambda^2 e) = J^T \tilde{F} \qquad (48)$$

Where:

$$\tilde{F} = (\hat{F} - F); \\ e = q - q_d \; ; \; \dot{e} = \dot{q} - \dot{q}_d \; ; \; \ddot{e} = \ddot{q} - \ddot{q}_d \qquad (49)$$

Also, Λ is the diagonal matrix described before.
Also, a sliding surface of s is defined through which the controlling input tries to guide the states within this error dynamic surface:

$$s = \dot{e} + \Lambda e; \\ \dot{s} = \ddot{e} + \Lambda\dot{e} \qquad (50)$$

Therefore, "Eq. (48)" can be rewritten according to s and its derivations:

$$D(\dot{s} + \Lambda s) = J^T \tilde{F} \qquad (51)$$

In order to determine $\hat{F}$ properly, The Lyapunov function is considered as follows:

$$V = \frac{1}{2}\left(s^T D s + \tilde{F}^T \Gamma \tilde{F}\right) \qquad (52)$$

Where D, Γ are the controlling gains related to the accuracy and controlling effort. D is the same inertia matrix, introduced in the motion equations of the system, And Γ is a determined diagonal matrix which specifies the importance of the external force estimation accuracy. also we have:

$$\dot{V} = s^T D \dot{s} + \tilde{F}^T \Gamma \dot{\tilde{F}} \qquad (53)$$

Extracting $\dot{s}$ from "Eq. (51)" and substituting the following $\dot{s}$ and $\dot{\tilde{F}}$ in "Eq. (53)" we have:

$$\dot{s} = D^{-1} J^T \tilde{F} - \Lambda s \qquad (54)$$

$$\dot{\tilde{F}} = \dot{\hat{F}} - \dot{F} = \dot{\hat{F}} \qquad (55)$$

$$\dot{V} = s^T D D^{-1}(J^T \tilde{F} - \Lambda s) + \tilde{F}^T \Gamma \dot{\hat{F}} = s^T J^T \tilde{F} - s^T \Lambda s + \\ \tilde{F}^T \Gamma \dot{\hat{F}} \qquad (56)$$

It can be seen that the Lyapunov function itself is always positive definite. Now it is enough to make its derivative negative definite by substituting a proper value for $\dot{\hat{F}}$. This parameter is selected as bellow:

$$\dot{\hat{F}} = -\Gamma^{-1} J s \qquad (57)$$

Thus, the derivation of the Lyapunov function becomes

semi-negative definite:

$$\dot{V} = -s^T \Lambda s \leq 0 \qquad (58)$$

By integrating $\dot{\hat{F}}$ with an initial guess, the parameter $\hat{F}$ can be substituted in the controlling signal of "Eq. (47)". Thus it can be concluded that using the mentioned controlling effort, not only the stability of the system can be assured, but also the sliding surface of "Eq. (51)" can be fellfield in the presence of external disturbances of firing action.

4   SIMULATION STUDY

In order to simulate the system, the specifications of "Table 2" are employed:

Table 2 The simulation parameters

symbol	Definition	value	Unit
g	Gravitational acceleration	9.81	$\frac{m}{s^2}$
m_w	Mass of each wheel	0.25	kg
m_b	Mass of mobile chassis	1.5	kg
m_1	Mass of the first link	0.3	kg
m_2	Mass of the second link	0.5	kg
m_3	Mass of the third link	0.5	kg
I_{wy}	The wheel's moment of inertia around Y axis of the global coordinate system	0.005	$kg.m^2$
I_{1z}	The first link's moment of inertia around the Z axis of the global coordinate system	0.005	$kg.m^2$
I_{2y}	The second link's moment of inertia around the Y axis of the global coordinate system	0.005	$kg.m^2$
I_{2z}	The second link's moment of inertia around the Z axis of the global coordinate system	0.005	$kg.m^2$
I_{3y}	The third link's moment of inertia around the Y axis of the global coordinate system	0.005	$kg.m^2$
I_{3z}	The third link's moment of inertia around the Z axis of the global coordinate system	0.005	$kg.m^2$
r	The radius of each wheel	0.15	m
d_1	Length of the first link	0.1	m
a_2	Length of the second link	0.2	m
a_3	Length of the third link	0.2	m
d_6	Length of the wrist	0.06	m
l	The height of the mobile chassis	0.23	m

In order to verify the correctness of modeling and efficiency of the proposed controlling system, the mobile manipulator is simulated in MATLAB-SIMULINK, and the proposed controller is implemented. Kinematics and kinetics of the system are simulated, and by comparing the actual and desired path of the tool through the inverse and direct model of the robot, the correctness of modeling is verified. Afterward, an external force resulted from the operational task is implemented on the end-effector and the actual behavior of the manipulator is compared between the proposed controlling strategy and the other conventional ones. Also, the superiority of the proposed adaptive force controller is investigated for firing applications.

4.1. Verification of Modeling

In this section, the correctness of the extracted kinematics and kinetics of the system is verified. Consider that the end-effector's velocity vector is supposed to track the following path of "Figs. 2 & 3":
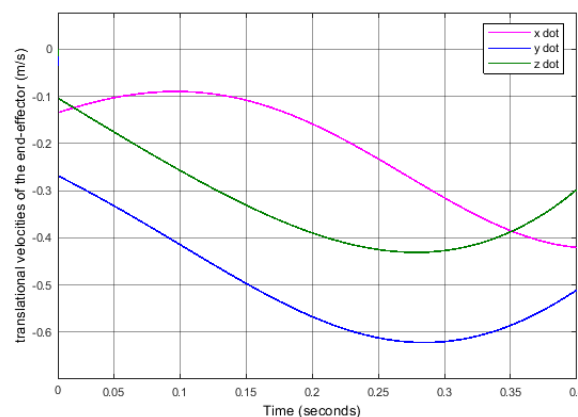
Fig. 2   Desired path of the end- effector's translational velocities.
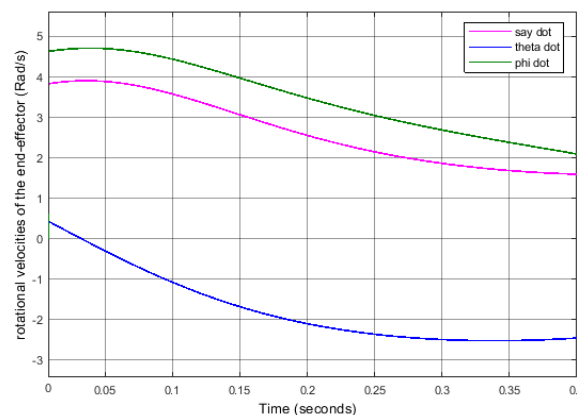
Fig. 3   Desired path of the end- effector's rotational velocities.

Using the formulation of kinematics explained in "Eqs. (8, 11)", required velocities of the robot joint space are

as follows in which the actual and desired paths are also compared ("Fig. 4"):
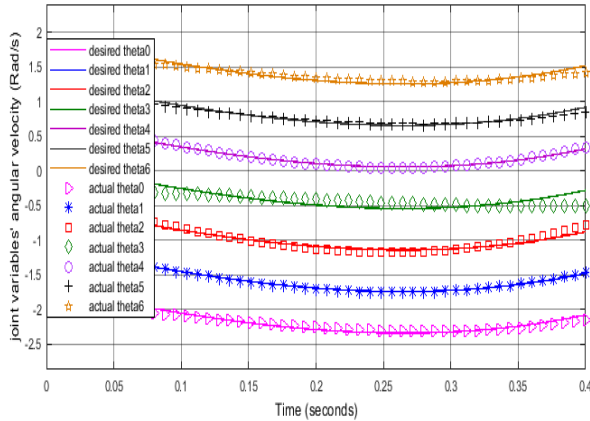
Fig. 4   comparison between the joint variables' angular velocity in the forward and inverse approach of kinematics.

As can be seen, the actual and desired path of the robot's joint space extracted through the inverse and direct kinematics are satisfactorily compatible which shows the correctness of kinematic modeling. Also for the desired trajectory of "Eqs. (59)", comparison of the desired and actual robot's joint space movement extracted from inverse and direct dynamics of the system is as "Fig. 5" for all of the joints. It should be mentioned that the desired path for each joint variable, is considered as a function of time according to radian as follows:

$$
\begin{aligned}
\theta_0 &= 5.2360t^2 - 7.8540t^3 + 3.1416t^4 & ; \\
\theta_1 &= 5.2360t^2 - 7.8540t^3 + 3.1416t^4 + 0.1 & ; \\
\theta_2 &= 5.2360t^2 - 7.8540t^3 + 3.1416t^4 + 0.2 & ; \\
\theta_3 &= 5.2360t^2 - 7.8540t^3 + 3.1416t^4 + 0.3 & (59)
\end{aligned}
$$
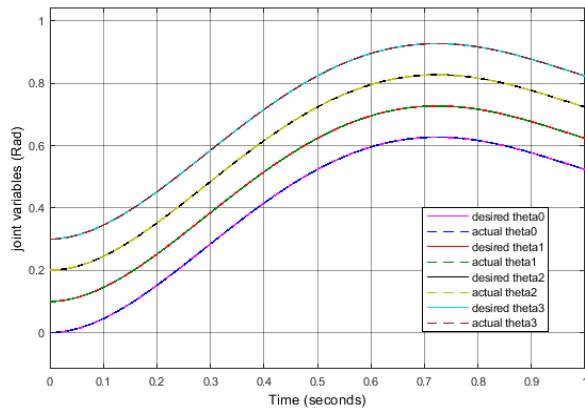
Fig. 5   Comparison between the desired and actual path for the joint variables extracted from the dynamic model of the system.

Again here the actual movement of the joints has a good accuracy compared to their desired paths which shows the correctness of the kinetic modeling of the robot.

Also, the required motors' torque of the robot joint for tracking the mentioned path is as "Fig. 6" which can be considered as the feedforward controlling term of the robot movement.
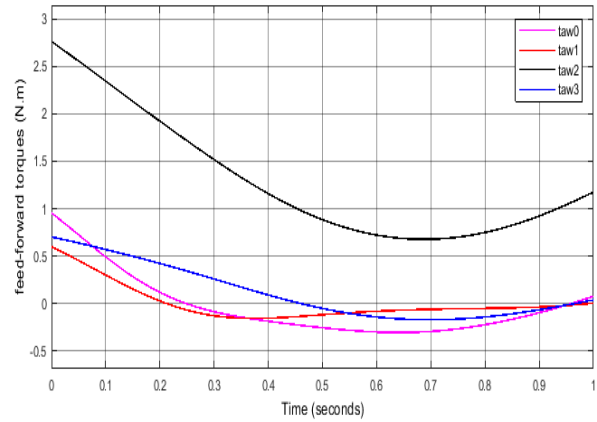
Fig. 6   Feedforward torque needed to track the desired path.

4.2. Verification of the Proposed Controller
As mentioned before, since the manipulator is supposed to perform an operational task, some external forces affect the end-effector which should be neutralized by the aid of the proposed force controller. In order to show the efficiency of the controller and ensure the stability and accuracy of the robot in this situation, some analytic and comparative scenarios are simulated in SIMULINK and the performance of different controlling strategies are compared.

The simplest controller is Feed-back Linearization (F.L.) for which no external force can be implemented. However it is shown here that since this method is a closed loop, both regulation and tracking can be performed simultaneously using this method. Consider the following initial condition for the robot through which the tracking of "Eq. (60)" should be conducted afterward:

$$
\theta_0 = \begin{cases} -0.225\cos(2\pi t) + 0.225 \ ; \ 0 \le t \le 0.5 \\ 0.45 \qquad\qquad\qquad\quad\ ; \ 0.5 < t \le 1 \end{cases} \quad (60)
$$

$$
\theta_1 = \theta_2 = \theta_3 = \begin{cases} 0.1 \qquad\qquad\qquad\quad\ ; \ 0 \le t \le 0.5 \\ \cos(2\pi t) + 0.225 \ ; \ 0.5 < t \le 1 \end{cases} \quad (61)
$$

$$
\theta(0) = \begin{bmatrix} 0.1 \\ 0.1 \\ 0.1 \\ 0.1 \end{bmatrix} \ ; \quad \dot{\theta}(0) = \begin{bmatrix} 0 \\ 0 \\ 0 \\ 0 \end{bmatrix} \quad (62)
$$

The response of the robots' joints and its comparison between inverse dynamics and F.L. relative to the desired path can be seen in "Fig. 7":
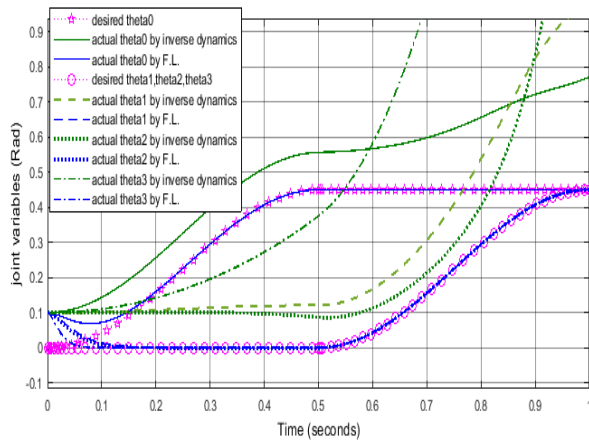
Fig. 7   Comparison between the desired and actual path by the inverse dynamic controller and F.L. controller.

It can be seen that contrary to the feed-forward approach in which the end-effector is deviated from the desired path, in the system in which F.L. is employed the regulation process is successfully done during the first 0.2 sec of movement and the rest of tracking is performed with good accuracy of about 289%. The workspace movement of the robot and its comparison between the mentioned controllers are depicted as follows ("Fig. 8"):
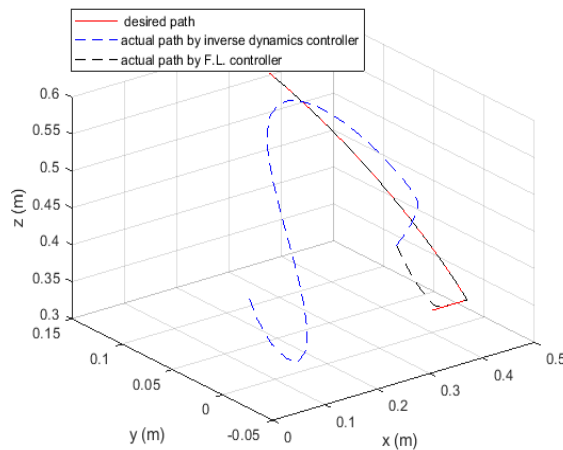
Fig. 8   Comparison between the desired and actual position of the end-effector by the inverse dynamic controller and Feed-back Linearization controller.

Required motor torque and its comparison between the mentioned controllers to guide the end-effector toward the path and maintain it within the desired path are extracted as "Fig. 9". The profile of the torque during the first 0.2 sec of movement is related to the regulation process during which an overshoot about 2 N.M can be observed in the profile of the torques.
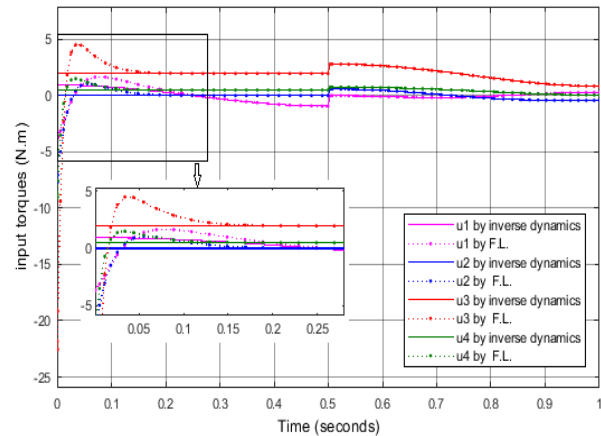
Fig. 9   Comparison of the required motors' torque for regulation and tracking the desired path using inverse dynamic and feedback linearization controller.

The rest variations of the torque profile, however, is related to the tracking process. Also, the observed increase in the torque profile of F.L. is the additional controlling effort to improve the tracking errors.

Now it is supposed that an external force and moment as mentioned in "Eqs. (63, 64)" is applied on the end-effector related to the operational task of the robot which cannot be controlled using a simple F.L. controller. Thus here an impedance control is added to the controlling effort in order to improve the stability and accuracy of the operation. Here since the external force is predetermined, impedance control can be applied to perform the operation. The External force and torque on the end-effector in N and N.m relatively is supposed as follows:

$$F = \begin{bmatrix} f_x \\ f_y \\ f_z \\ M_x \\ M_y \\ M_z \end{bmatrix} \tag{63}$$

Where:

$$f_x = f_y = f_z = M_x = M_y = M_z$$
$$= \begin{cases} 0 & ; \quad 0 \le t < 0.6 \\ 2 & ; \ 0.6 \le t < 0.8 \\ 0 & ; \qquad t \ge 0.8 \end{cases} \tag{64}$$

The desired path considered in "Eq. (60)" related to the previous maneuver and its comparison between the actual path by the simple F.L. and impedance controller are depicted in "Fig. 10":
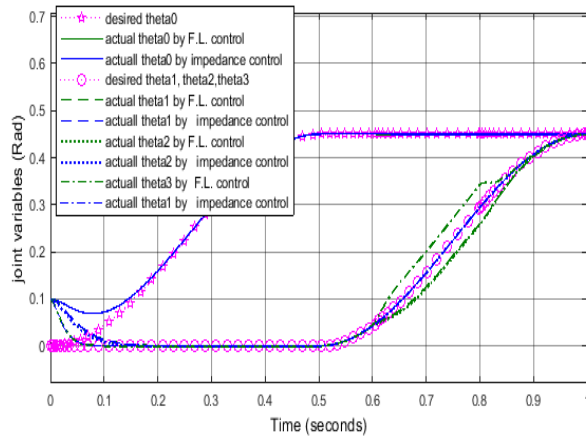
Fig. 10 Actual joint space response of the robot in the presence of external forces and moments and its comparison between the actual path by F.L. and impedance controllers.

Here again it can be seen that the system which is controlled using impedance control, can successfully accomplish both of regulation and tracking in a good way whereas the end-effector in the system in which a simple F.L. is employed deviates from its desired path, and this fact shows the superiority of the impedance controller for the processes in which an external force is engaged during an operational task. Here the improvement of tracking is about 7% which is significantly a high modification. The workspace movement of the robot and its comparison between the mentioned controllers is depicted as follows ("Fig. 11"):
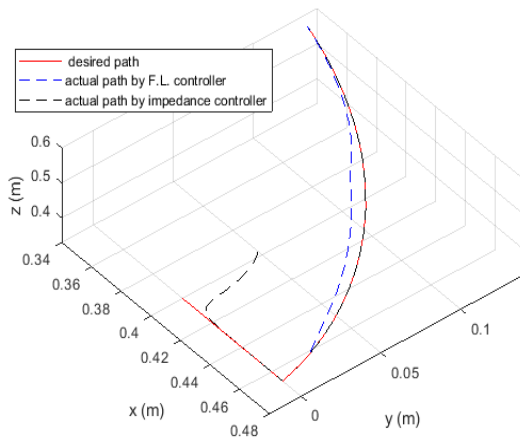
Fig. 11 Comparison between the desired and actual position of the end-effector equipped by feedback linearization controller and impedance controller.

The required motors' torque using this improved controlling strategy and its comparison with the simple F.L. can be seen as follows ("Fig. 12"). The changes in the torque profile of impedance control relative to F.L. are required for neutralizing the effect of external force.
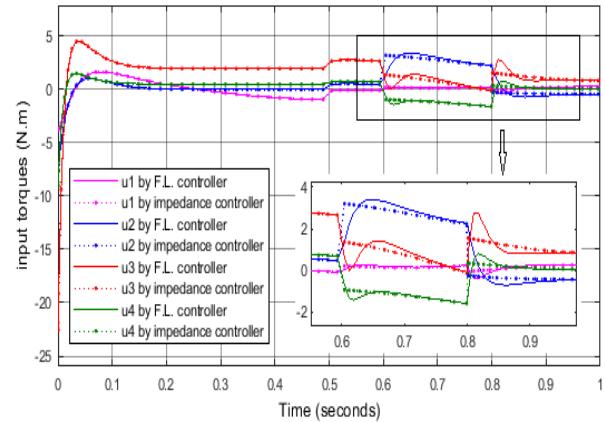
Fig. 12 comparison of the required motors' torques in the presence of external forces between feedback linearization controller and impedance controller.

Now it is supposed that the external force is contributed to the firing process and is not predetermined, so a simple force control cannot be used and the external force needs to be estimated using the proposed adaptive controller. The external force is considered as mentioned in "Eqs. (63, 64)".
Here the controlling gains related to the adaptive controller are tuned as bellow to achieve a good response:

$$\Lambda = \begin{bmatrix} 25 & 0 & 0 & 0 \\ 0 & 35 & 0 & 0 \\ 0 & 0 & 40 & 0 \\ 0 & 0 & 0 & 80 \end{bmatrix};$$

$$\Gamma = \begin{bmatrix} 0.001 & 0 & 0 & 0 & 0 & 0 \\ 0 & 0.002 & 0 & 0 & 0 & 0 \\ 0 & 0 & 0.001 & 0 & 0 & 0 \\ 0 & 0 & 0 & 1 & 0 & 0 \\ 0 & 0 & 0 & 0 & 0.005 & 0 \\ 0 & 0 & 0 & 0 & 0 & 0.005 \end{bmatrix} \tag{65}$$

The initial guess of the external force and moment domain is:

$$\hat{F}(0) = \begin{bmatrix} \hat{f}_x(0) \\ \hat{f}_y(0) \\ \hat{f}_z(0) \\ \widehat{M}_x(0) \\ \widehat{M}_y(0) \\ \widehat{M}_z(0) \end{bmatrix} = \begin{bmatrix} 2.25 \\ 2.25 \\ 2.25 \\ 2.25 \\ 2.25 \\ 2.25 \end{bmatrix} \tag{66}$$

Which is also considered as the external force vector input to the controller of "Eq. (45)" in order to compare the efficiency of two recent controlling methods.
The joint space response of the robot in the presence of the undetermined external force for the previously

desired maneuver of the robot is as "Fig. 13", and this path is compared for two controlling strategies of impedance controller and proposed adaptive force controller.
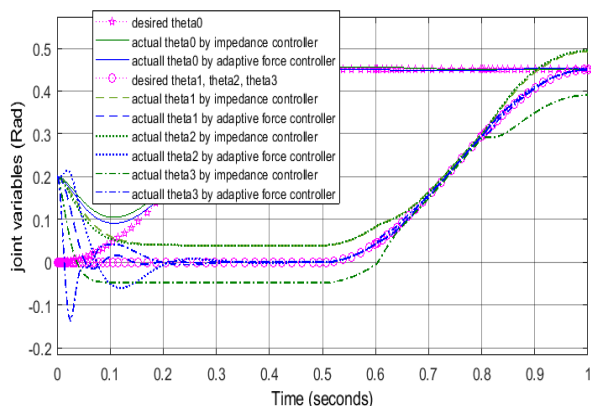
Fig. 13   Actual joint space response of the robot in the presence of external forces and its comparison between impedance force controller and adaptive force controller.

Here the initial guess of adaptive force controller is considered as the external force of the impedance controller, and it can be seen that this guess is improved in the adaptive controller whereas it is not improved for impedance controller. Consequently, the impedance controller in which the initial guess of the external force is substituted as the external force has failed to perform the proper maneuver whereas the proposed adaptive controller has successfully performed the regulation and tracking by proper estimation of the external force. It can be seen that over 8.5% improvement in accuracy can be observed using the proposed adaptive controller. The desired workspace movement of the robot and its comparison between the mentioned controllers is depicted as follows ("Fig. 14"):
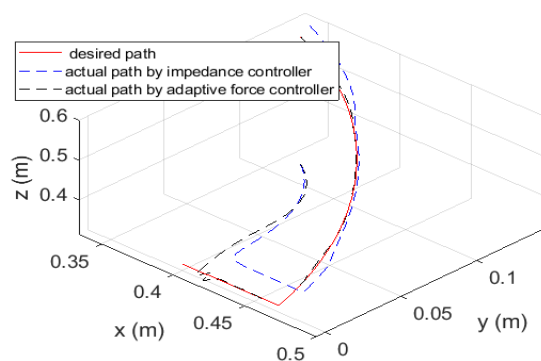
Fig. 14   Comparison between the desired and actual position of the end-effector equipped by impedance and adaptive force controllers.

The corresponding required motors' torque, and its comparison for these controllers can be seen in "Fig. 15".
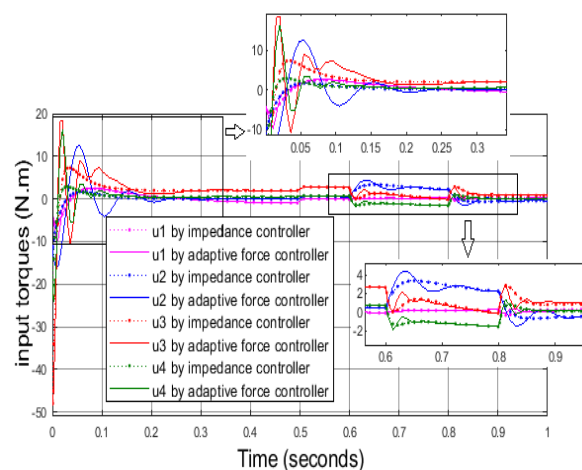
Fig. 15   Required motors' torque of the robot in the presence of external forces and its comparison between the impedance and adaptive force controllers.

Again here the variations of the torque during the time is improved for the proposed controller in a way that the actual applied force on the end-effector which is time-dependent can be precisely estimated and neutralized. In the following figure, the estimated force which is evaluated by the controller can be seen ("Fig. 16").
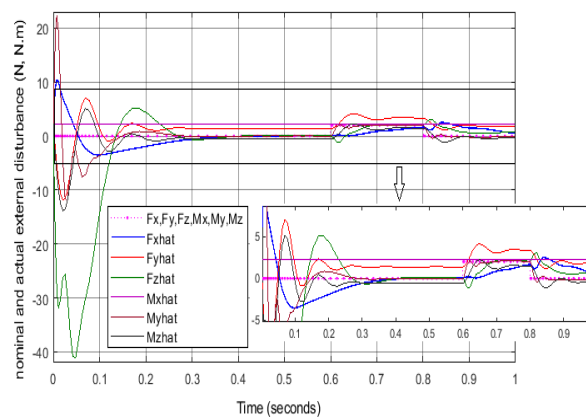
Fig. 16   The estimated force of the adaptive controller.

It can be seen that the initial guess of the force is improved toward the actual value of the implemented force and has converged to a steady state near the actual value of the external force which shows the efficiency of the proposed adaptive force controller. Thus it can be concluded that for our case of study, which is a mobile manipulator with firing application, the sole applicable and efficient method of controlling which can successfully perform the tracking and operational task simultaneously is the proposed adaptive force controller and the rest of traditional controllers have failed to perform the process.

5   CONCLUSION

In this paper, a new mobile manipulator is designed and modeled by which firing task can be performed and thus is exposed to external forces. An adaptive force control was proposed to control the motion and operation of this robot, and the efficiency of this controller was compared with the conventional controlling approach. Kinematics and kinetics of the robot were extracted as the main perquisites of controlling the system. Afterward three different controllers including F.L., impedance control and adaptive force controller were designed and implemented on the robot, and their performances were investigated.

The correctness of modeling was verified by comparing the actual and desired paths of inverse and direct models. Also, the efficiency of the proposed force controller toward neutralizing the destructive effect of external forces was illustrated by the aid of conducting some comparative and analytic simulation scenarios. It was seen that for the cases in which no external force is applied on the end-effector, FL could perform the regulation and tracking with a good accuracy which is 289% better than feed-forward approach. However, when an external force is exerted on the end effector as a result of an operational task, the actual path of the system controlled by simple F.L. deviates from its desired one, and it is required to add the controlling term related to force control.

Here the impedance controller can improve the tracking and operation of the robot by about 7%. Moreover, it was seen that this force control again is just applicable and efficient in the cases that the external force is entirely predetermined. For the cases in which the external force is unknown, like for the case of firing actions, it was seen that even this method is not properly efficient. Therefore, a new method of adaptive force control was proposed and developed in this paper through which the external force related to firing is considered as an external disturbance and the value of this force can be estimated by the controller and its related controlling motors' torque is calculated and implemented by the motors. As a result, it was seen that by implementing the designed adaptive controller, not only the robot motion can be done with a good accuracy (about 8.5% improvement), but also its related operating task which is firing action, in this case, can be accomplished while the stability of the robot is guaranteed and the targeting process can be done with a good accuracy.

LIST OF SYMBOLS

symbol	Definition
g	Gravitational acceleration
m_w	Mass of each wheel
m_b	Mass of mobile chassis
m_1	Mass of the first link
m_2	Mass of the second link
m_3	Mass of the third link
I_{wy}	The wheel's moment of inertia around the Y axis of the global coordinate system
I_{1z}	The first link's moment of inertia around the Z axis of the global coordinate system
I_{2y}	The second link's moment of inertia around the Y axis of the global coordinate system
I_{2z}	The second link's moment of inertia around the Z axis of the global coordinate system
I_{3y}	The third link's moment of inertia around the Y axis of the global coordinate system
I_{3z}	The third link's moment of inertia around the Z axis of the global coordinate system
r	The radius of each wheel
d_1	Length of the first link
a_2	Length of the second link
a_3	Length of the third link
d_6	Length of the wrist
l	The height of the mobile chassis
x	The first global coordinate of the end-effector's position
y	The second global coordinate of the end-effector's position
z	The third global coordinate of the end-effector's position
ψ	The first global coordinate of the end-effector's orientation
θ	The second global coordinate of the end-effector's orientation
φ	The third global coordinate of the end-effector's orientation
θ_0	The 1st joint space variable
θ_1	The 2nd joint space variable
θ_2	The 3rd joint space variable
θ_3	The 4th joint space variable
θ_4	The 5th joint space variable
θ_5	The 6th joint space variable
θ_6	The 7th joint space variable
J	Jacobian matrix of the kinematic model
p	Vector of the work space variables
q	Vector of the join space variables
$\dot{p}$	The velocity vector of the work space variables
$\dot{q}$	The velocity vector of the joint space variables
T_w	The kinetic energy of each wheel
V_w	The translational velocity vector of each wheel's center of mass
ω_w	The rotational velocity vector of each wheel's center of mass
I_w	Each wheel's Moment of inertia matrix according to the global coordinate system
U_w	The potential energy of each wheel
U_b	The potential energy of the mobile chassis
U_1	The potential energy of the first link
U_2	The potential energy of the second link
U_3	The potential energy of the third link

T_b	The kinetic energy of the mobile chassis
V_b	The translational velocity vector of the mobile chassis center of mass
T_1	The kinetic energy of the first link
V_1	The translational velocity vector of the first link's center of mass
ω_1	The rotational velocity vector of the first link
I_1	The first link's Moment of inertia matrix according to the global coordinate system
T_2	The kinetic energy of the second link
V_2	The translational velocity vector of the second link's center of mass
ω_2	The rotational velocity vector of the second link
I_2	The second link's moment of inertia matrix according to the global coordinate system
T_3	The kinetic energy of the third link
V_3	The translational velocity vector of the third link's center of mass
ω_3	The rotational velocity vector of the third link
I_3	The third link's moment of inertia matrix according to the global coordinate system
$\dot{\theta}_0$	The first joint's rate of variation
$\dot{\theta}_1$	The second joint's rate of variation
$\dot{\theta}_2$	The third joint's rate of variation
$\dot{\theta}_3$	The fourth joint's rate of variation
L	Lagrangian of the system
T_{total}	The kinetic energy of the system
U_{total}	The potential energy of the system
τ_0	The first joint's coordinate force
τ_1	The second joint's generalized force
τ_2	The third joint's generalized force
τ_3	The fourth joint's generalized force
τ	Generalized force vector
D	The inertia matrix of the system
C	The coriolis matrix of the system
G	The gravity matrix of the system
q	The joint space variables vector
$\dot{q}$	The joint space variables velocity vector
$\ddot{q}$	The joint space variables acceleration vector
$\ddot{\theta}_0$	The first joint variable acceleration
$\ddot{\theta}_1$	The second joint variable acceleration
$\ddot{\theta}_2$	The third joint variable acceleration
$\ddot{\theta}_3$	The fourth joint variable acceleration
$\boldsymbol{x}$	State vector
x_1	The 1st state variable
x_2	The 2nd state variable
x_3	The 3rd state variable
x_4	The 4th state variable
x_5	The 5th state variable
x_6	The 6th state variable
x_7	The 7th state variable
x_8	The 8th state variable
u	Joint input vector
u_1	The first joint input
u_2	The second joint input
u_3	The third joint input
u_4	The fourth joint input

K	The inverse of matrix D
x_0	The operating point which in the controllability of the system is investigated
u_0	input vector related to the operating point
$\dot{x}$	Vector of the state space equations
A	
B	
f	The nonlinear function of state space
φ_C	Controllability matrix
q_d	Desired position path of joint space vector
$\dot{q}_d$	Desired velocity path of joint space vector
$\ddot{q}_d$	Desired acceleration path of joint space vector
Λ	Controlling gain matrix
e	The position tracking error vector
$\dot{e}$	The velocity tracking error vector
$\ddot{e}$	The acceleration tracking error vector
F	The actual external force and torque vector
F_x	The external force applied to the end-effector in the positive direction of the global X axis
F_y	The external force applied to the end-effector in the positive direction of the global Y axis
F_z	The external force applied to the end-effector in the positive direction of the global Z axis
M_x	The external torque applied to the end-effector about the positive direction of the global X axis
M_y	The external torque applied to the end-effector about the positive direction of the global Y axis
M_z	The external torque applied to the end-effector about the positive direction of the global Z axis
$\hat{F}$	The nominal external force and torque vector
$\tilde{F}$	Difference between the actual and nominal external force and torque vector
s	The sliding surface defined as a function of e, $\dot{e}$ and Λ
Γ	Controlling gain matrix
t	time

REFERENCES

[1] Jakubiak, J., Małek, Ł., and Tchoń, K., A New Inverse Kinematics Algorithm for Nonholonomic Mobile Robots, IFAC Proceedings Vol.42. No. 13, 2009, pp. 647-652.

[2] Trojnacki, M., Dąbek, P., Studies of Dynamics of a Lightweight Wheeled Mobile Robot During Longitudinal Motion on Soft Ground, Mechanics Research Communications, Vol. 82, 2017, pp. 36-42.

[3] Khanpoor, A., Khalaji, A. K., and Moosavian, S. A. A., Dynamics Modeling and Control of a Wheeled Mobile Robot with Omni-Directional Trailer, In Electrical Engineering (ICEE), 2014 22nd Iranian Conference on. 2014. IEEE.

[4] Sharma, A., Panwar, V., Control of Mobile Robot for Trajectory Tracking by Sliding Mode Control Technique. in Electrical, Electronics, and Optimization Techniques (ICEEOT), International Conference on. 2016. IEEE.

[5] Hassanzadeh, I., Madani, K., and Badamchizadeh, M. A., Mobile Robot Path Planning Based on Shuffled Frog Leaping Optimization Algorithm, In Automation Science and Engineering (CASE), IEEE Conference on, 2010. IEEE.

[6] Shojaei, K., Shahri, A. M., and Tarakameh, A., Adaptive Feedback Linearizing Control of Nonholonomic Wheeled Mobile Robots in Presence of Parametric and Nonparametric Uncertainties, Robotics and Computer-Integrated Manufacturing, Vol. 27, No. 1, 2011, pp. 194-204.

[7] Chen, Y. H., Li, T. H. S. and Chen, Y. Y., A Novel Nonlinear Control Law with Trajectory Tracking Capability for Nonholonomic Mobile Robots: Closed-form Solution Design, Applied Mathematics & Information Sciences, Vol. 7, No. 2, 2013, pp. 749.

[8] Koubaa, Y., Boukattaya, M., and Dammak, T., Adaptive Control of Nonholonomic Wheeled Mobile Robot with Unknown Parameters, In Modelling, Identification and Control (ICMIC), 7th International Conference on, 2015, IEEE.

[9] Korayem, M., Shafei, A., Motion Equation of Nonholonomic Wheeled Mobile Robotic Manipulator with Revolute–Prismatic Joints Using Recursive Gibbs–Appell Formulation, Applied Mathematical Modelling, Vol. 39, No, 5-6, 2015, pp. 1701-1716.

[10] Seidi, E., et al. Dynamic Modeling and Parametric Analysis of Dual Arm Manipulator with Revolute-Prismatic Joints Mounted on a Nonholonomic Mobile Base, In Robotics and Mechatronics (ICROM), 3rd RSI International Conference on, 2015, IEEE.

[11] Korayem, M., et al., Analysis and Experimental Study of Non-Holonomic Mobile Manipulator in Presence of Obstacles for Moving Boundary Condition, Acta Astronautica, Vol. 67, No. 7-8, 2010, pp. 659-672.

[12] Korayem, M., Shafei, A., and Seidi, E., Symbolic Derivation of Governing Equations for Dual-Arm Mobile Manipulators Used in Fruit-Picking and the Pruning of Tall Trees, Computers and Electronics in Agriculture, Vol. 105, 2014, pp. 95-102.

[13] Deepak, B., Parhi, D. R. and Praksh, R., Kinematic Control of a Mobile Manipulator. in Proceedings of the International Conference on Signal, Networks, Computing, and Systems. 2016. Springer.

[14] Boukens, M., Boukabou, A., and Chadli, M., Robust Adaptive Neural Network-Based Trajectory Tracking Control Approach for Nonholonomic Electrically Driven Mobile Robots, Robotics and Autonomous Systems, Vol. 92, 2017, pp. 30-40.

[15] Djebrani, S., Benali, A., and Abdessemed, F., Impedance Control of an Omnidirectional Mobile Manipulator, IFAC Proceedings Vol. 42, No. 13, 2009, pp. 519-524.

[16] Lippiello, V., Ruggiero, F., Cartesian Impedance Control of a UAV with a Robotic Arm. 2012.

[17] Wang, Y., Mai, T., and Mao, J., Adaptive Motion/Force Control Strategy for Non-Holonomic Mobile Manipulator Robot Using Recurrent Fuzzy Wavelet Neural Networks, Engineering Applications of Artificial Intelligence, Vol. 34, 2014, pp. 137-153.

[18] Yin, X., Pan, L., Enhancing Trajectory Tracking Accuracy for Industrial Robot with Robust Adaptive Control, Robotics and Computer-Integrated Manufacturing, Vol. 51, 2018, pp. 97-102.

[19] Gracia, L., et al., Adaptive Sliding Mode Control for Robotic Surface Treatment Using Force Feedback, Mechatronics, Vol. 52, 2018, pp. 102-118.

[20] Fedaravičius, A., Ragulskis, M., and Sližys, E., Dynamic Synthesis of the Recoil Imitation System of Weapons, Mechanics, Vol. 51, No. 1, 2005, pp. 44-48.

[21] Spong, M.W., Hutchinson, S., and Vidyasagar, M., Robot Modeling and Control, 2006.

[22] Slotine, J. J. E., Li, W., Applied Nonlinear Control. Vol. 199. 1991: Prentice hall Englewood Cliffs, NJ.

[23] Schilling, R. J., Fundamentals of Robotics: Analysis and Control, Vol. 629. 1990: Prentice Hall New Jersey.